Computation of inflationary cosmological perturbations in chaotic inflationary scenarios using the phase-integral method

Clara Rojas[1,*] and Víctor M. Villalba[2,†]

[1]*Departamento de Física, Aplicada IVIC/Mérida, Mérida 5107, Venezuela*
[2]*Centro de Física IVIC Apdo 21827, Caracas 1020A, Venezuela*

(Received 4 September 2007; revised manuscript received 5 March 2009; published 1 May 2009)

The phase-integral approximation devised by Fröman and Fröman is used for computing cosmological perturbations in the quadratic chaotic inflationary model. The phase-integral formulas for the scalar and tensor power spectra are explicitly obtained up to fifth order of the phase-integral approximation. We show that the phase integral gives a very good approximation for the shape of the power spectra associated with scalar and tensor perturbations as well as the spectral indices. We find that the accuracy of the phase-integral approximation compares favorably with the numerical results and those obtained using the slow-roll and uniform-approximation methods.

DOI: 10.1103/PhysRevD.79.103502 PACS numbers: 98.80.Cq, 03.65.Sq, 05.45.Mt

I. INTRODUCTION

The study of the spectrum of anisotropies of the cosmic microwave background radiation and inhomogeneities in the large scale structure of the Universe provides key elements in the study of the early universe. The results reported by WMAP favor inflation [1–3] over other cosmological scenarios. The present and future observational data will permit us to validate and discriminate among different inflationary models. According to WMAP5 data the power-law inflation, the hybrid inflation, and quartic chaotic inflationary models $\lambda\phi^4$ are ruled out, while the quadratic chaotic inflationary model $m^2\phi^2$ agreed with the observational data [1,4].

In order to compare with observations, we should be able to obtain very accurate results for the predicted power spectrum of primordial perturbations for a variety of inflationary scenarios. In general, most of the inflationary models are not exactly solvable and approximate or numerical methods are mandatory in the computation of the scalar and power spectra. Traditionally, the method of approximation applied in inflationary cosmology is the slow-roll approximation [5], which produces reliable results in inflationary models with smooth potentials, but cannot be improved in a simple way beyond the leading order. Recently, some authors have applied alternative approximations, such as the WKB method with the Langer modification [6–8], the Green function method [9], and the improved WKB method [10,11].

Habib *et al.* [12–14] have successfully applied the uniform-approximation method in the calculation of the scalar and tensor power spectra and the corresponding spectral indices for the quadratic and quartic chaotic inflationary models, showing that the uniform approximation gives more accurate results than the slow-roll approximation. Casadio *et al.* [15] have applied the method of comparison equation to study cosmological perturbations during inflation. The comparison method is based on the uniform approximation proposed by Dingle [16] and Miller [17] and thoroughly discussed by Berry and Mount [18].

Recently [19,20], the phase-integral approximation [21–23] has been applied to the calculation of the power spectra and spectral indices in the power-law inflationary model, showing that the phase-integral method gives results which are comparable or better than those obtained using slow roll or the uniform approximation. It is the purpose of this paper to compute approximate solutions for the scalar and tensor power spectra and their corresponding spectral indices for some chaotic inflationary models with the help of the phase-integral approximation method. We show that for the quadratic chaotic inflationary model the fifth-order phase-integral approximation gives more accurate results than those obtained using the WKB or uniform-approximation methods. For the quartic chaotic inflationary model we also obtain very accurate results but we do not report them since this model is ruled out by the observational data [1].

The article is structured as follows: In Sec. II we apply the phase-integral approximation to the chaotic quadratic inflationary model, we numerically solve the equation governing the scalar and tensor perturbations, and we compare the results for the power-spectra obtained using the phase-integral approach with those computed with the slow-roll and uniform-approximation methods. In Sec. III we summarize our results.

II. PHASE-INTEGRAL APPROXIMATION FOR THE POWER SPECTRUM IN THE ϕ^2 CHAOTIC INFLATION

In this section we discuss the application of the phase-integral approximation to the computation of the power

*clararoj@gmail.com
†villalba@ivic.ve

spectrum in the chaotic inflationary $\frac{1}{2}m^2\phi^2$ model. We apply the phase-integral approximation in the study of the evolution of the mode k equations for the scalar and tensor perturbations in order to compute the scalar and tensor power spectra. Using the fifth-order phase-integral approximation we compute the scalar and tensor power spectra and their corresponding spectral indices. A detailed description of the method is given in Refs. [19,20].

A. The model

The chaotic inflationary model was introduced by Linde [24,25]. He proposed that the preinflationary universe was chaotic which means that the fields would take different values in different points of the space following a random pattern and inflation will occur in virtually any universe that begins in a chaotic, high energy state and has a scalar field with unbounded potential energy. The simplest form of the inflaton potential $V(\phi)$ in a chaotic model is given by the quadratic potential

$$V(\phi) = \tfrac{1}{2}m^2\phi^2, \tag{1}$$

giving as a result a free scalar field with mass m.

B. Equations of motion

In an inflationary universe driven by a scalar field, the equations of motion for the inflaton ϕ and the Hubble parameter H are given by

$$\ddot{\phi} + 3H\dot{\phi} = -\frac{\partial V(\phi)}{\partial \phi}, \tag{2}$$

$$H^2 = \frac{1}{3M_{\rm Pl}^2}\left[V(\phi) + \frac{1}{2}\dot{\phi}^2\right], \tag{3}$$

where the dots indicate derivatives with respect to physical time t. In the quadratic chaotic inflationary model Eqs. (2) and (3) are not exactly solvable in closed form; they can be solved numerically or using the slow-roll approximation. In the slow-roll approximation [26] we consider that the scalar field $V(\phi)$ varies very slowly $\frac{1}{2}\dot{\phi}^2 \ll V(\phi)$. Using this approximation, we obtain that Eqs. (2) and (3) for the quadratic chaotic inflationary model reduce to [27]

$$3H\dot{\phi} \simeq -m^2\phi, \tag{4}$$

$$H \simeq \frac{m\phi}{\sqrt{6}M_{\rm Pl}}. \tag{5}$$

Using Eqs. (4) and (5) we obtain that, in the slow-roll approximation, the expansion factor $a(t)$ and the inflaton field $\phi(t)$ are

$$\phi_{\rm sr} \simeq \phi_i - \sqrt{\frac{2}{3}}mM_{\rm Pl}t, \tag{6}$$

$$a_{\rm sr} \simeq a_i \exp\left(\frac{m\phi_i}{\sqrt{6}M_{\rm Pl}}t - \frac{m^2}{6}t^2\right), \tag{7}$$

where ϕ_i is a constant of integration corresponding to the initial value of the inflaton. Equation (7) shows that the Universe expands exponentially during inflation The slow-roll parameter is [9]

$$\epsilon_1 = \frac{\dot{H}}{H^2} = \frac{2M_{\rm Pl}^2}{\phi^2}. \tag{8}$$

The inflationary epoch finishes when $\epsilon_1 = 1$, that is $\phi_f = \sqrt{2}M_{\rm Pl}$, when the scalar field starts to oscillate. The mass m of the inflation can be fixed using the amplitude of the density fluctuations detected by WMAP. In order to fit m to the observational data, we demand that $m \simeq 10^{-6}$ [3].

The equations of motion (2) and (3) are numerically integrated in the physical time t. We solve the system of coupled differential equations (2) and (3) with the help of the sixth-order Runge-Kutta method [28], which can be written as

$$\begin{aligned} \ddot{\phi} + 3\frac{\dot{a}}{a}\dot{\phi} + \frac{\partial V(\phi)}{\partial \phi} &= 0, \\ \frac{\dot{a}}{a} - \sqrt{6}M_{\rm Pl}[2V(\phi) + \dot{\phi}^2]^{1/2} &= 0. \end{aligned} \tag{9}$$

We choose the initial value of the inflaton as $\phi_i = 15.4M_{\rm Pl}$. Since the evolution of the inflation ϕ is governed by a second-order differential equation, we need to fix the initial value for the velocity of the scalar field $\dot{\phi}_i$, which can be obtained using the slow-roll approximation (6). The initial value for a_i is chosen as $a_i = 1$, the mass of the inflaton $m^2 = 1.89 \times 10^{-12}M_{\rm Pl}^2$. The initial condition has been selected in order to guarantee enough inflation. In order to find the number of e-folds, we rewrite the system of differential equations (9) as

$$\begin{aligned} \ddot{\phi} + 3\dot{N}\dot{\phi} + \frac{\partial V(\phi)}{\partial \phi} &= 0, \\ \dot{N} &= \sqrt{6}M_{\rm Pl}[2V(\phi) + \dot{\phi}^2]^{1/2}. \end{aligned} \tag{10}$$

We find that the inflation finishes at $t_f = 1.30 \times 10^7 M_{\rm Pl}^{-1} = 3.51 \times 10^{-36}$ s, a result that corresponds to 59.84 e-folds before the scalar field starts to oscillate. Figure 1 shows the evolution of the scalar field ϕ.

In order to apply the phase-integral approximation to higher orders it is necessary to calculate the integrals $\omega(z)$ in the complex plane; therefore, it is of help to have an analytic expression for $a(t)$ and $\phi(t)$ which can be obtained after fitting the numerical data. We find that $a(t)$ and $\phi(t)$ take the form

$$a(t) = a_i \exp(\alpha t - \beta t^2), \tag{11}$$

$$\phi(t) = \gamma - \sigma t, \tag{12}$$

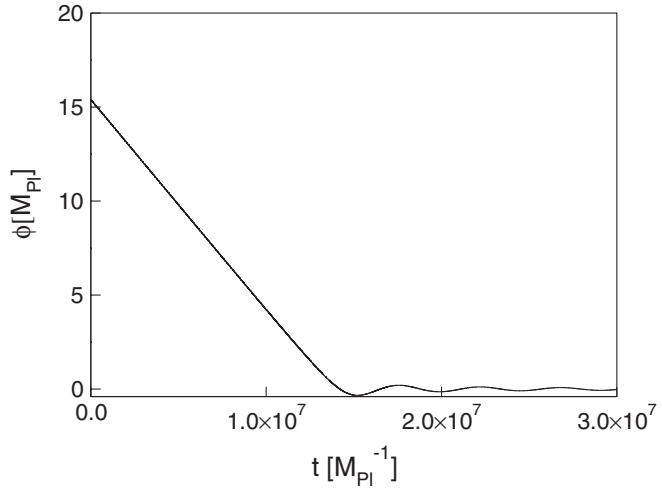

FIG. 1. Evolution of the potential ϕ for the chaotic inflationary model $\frac{1}{2}m^2\phi^2$.

where $\alpha = 8.6551 \times 10^{-6} M_{\rm Pl}$, $\beta = 3.1380 \times 10^{-13} M_{\rm Pl}^2$, $\gamma = 15.3992 M_{\rm Pl}$, and $\sigma = 1.1201 \times 10^{-6} M_{\rm Pl}^2$. With the help of the expressions (11) and (12) we obtain that $z_{\rm S}$ is given by

$$z_{\rm S}(t) = -\frac{a_i \gamma}{(\alpha - 2\beta t)} \exp(\alpha t - \beta t^2). \tag{13}$$

Figures 2(a) and 2(b) compare the fitting with the numerical result and the slow-roll approximations for $a(t)$ and $\phi(t)$. The fitting is valid up to $t = 5.00 \times 10^6 M_{\rm Pl}^{-1}$. The inset is an enlargement of the figure. Figures 3(a) and 3(b) show the ratio of the fit and slow roll to exact solution for $a(t)$ and $\phi(t)$ and observe that the fitting better approximates the numerical result than the slow-roll approximation; therefore the expressions for the scalar and tensor perturbations will be constructed using the fitting $a(t)$ and $z_{\rm S}(t)$ given by expressions (11) and (13), respectively. If we use $a_{\rm sr}$ and $\phi_{\rm sr}$ in order to calculate the power spectrum, the expression we obtain does not approach the exact result.

C. Equation for the perturbations

Since the expansion factor a and the field ϕ exhibit a simpler form in the physical time t than in the conformal time η, we proceed to write the equations for the scalar and tensor perturbations in the variable t. The relation between t and η is given via the equation $dt = ad\eta$. In this case, the equation for the perturbations can be written as

$$\ddot{u}_k + \frac{\dot{a}}{a}\dot{u}_k + \frac{1}{a^2}\left[k^2 - \frac{(\dot{a}\dot{z}_{\rm S} + a\ddot{z}_{\rm S})a}{z_{\rm S}}\right]u_k = 0, \tag{14}$$

$$\ddot{v}_k + \frac{\dot{a}}{a}\dot{v}_k + \frac{1}{a^2}[k^2 - (\dot{a}^2 + a\ddot{a})]v_k = 0. \tag{15}$$

In order to apply the phase-integral approximation, we eliminate the terms $\dot{u}_k$ and $\dot{v}_k$ in Eqs. (14) and (15). We

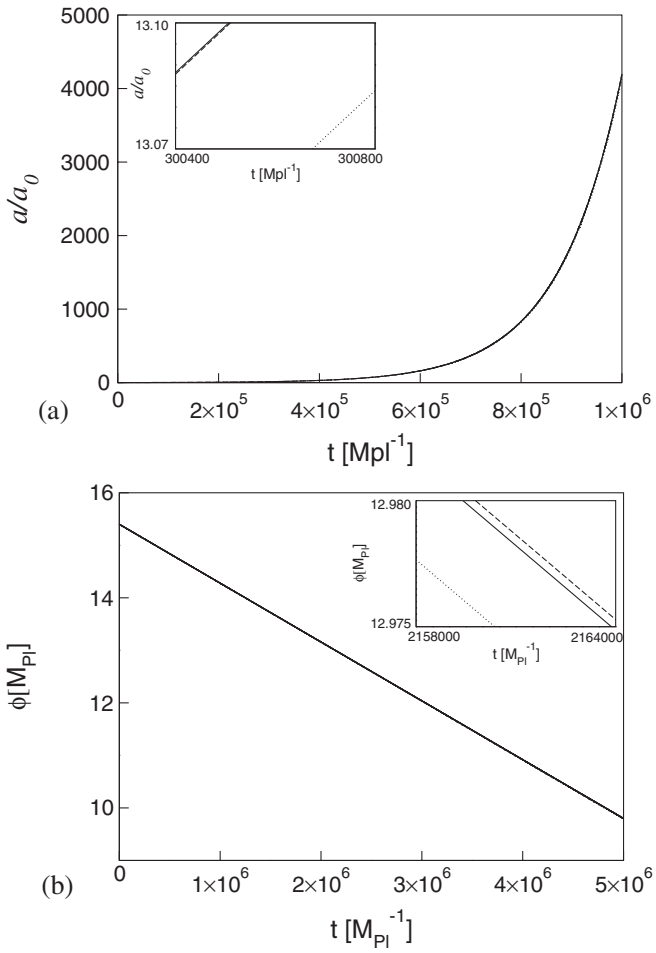

FIG. 2. (a) Evolution of the scale factor a and (b) evolution of the inflaton ϕ for the chaotic inflationary model $\frac{1}{2}m^2\phi^2$. Solid lines: numerical solution; dashed lines: fitting; dotted lines: slow-roll approximation. The inset is an enlargement of the figure.

make the change of variables $u_k(t) = \frac{U_k(t)}{\sqrt{a}}$ and $v_k(t) = \frac{V_k(t)}{\sqrt{a}}$, obtaining that U_k and V_k satisfy the differential equations:

$$\ddot{U}_k + R_{\rm S}(k,t)U_k = 0, \tag{16}$$

$$\ddot{V}_k + R_{\rm T}(k,t)V_k = 0, \tag{17}$$

with

$$R_{\rm S}(k,t) = \frac{1}{a^2}\left[k^2 - \frac{(\dot{a}\dot{z}_{\rm S} + a\ddot{z}_{\rm S})a}{z_{\rm S}}\right] + \frac{1}{4a^2}(a^2 - 2a\ddot{a}), \tag{18}$$

$$R_{\rm T}(k,t) = \frac{1}{a^2}[k^2 - (\dot{a}^2 + a\ddot{a})] + \frac{1}{4a^2}(a^2 - 2a\ddot{a}), \tag{19}$$

where $U(k)$ satisfies the asymptotic conditions

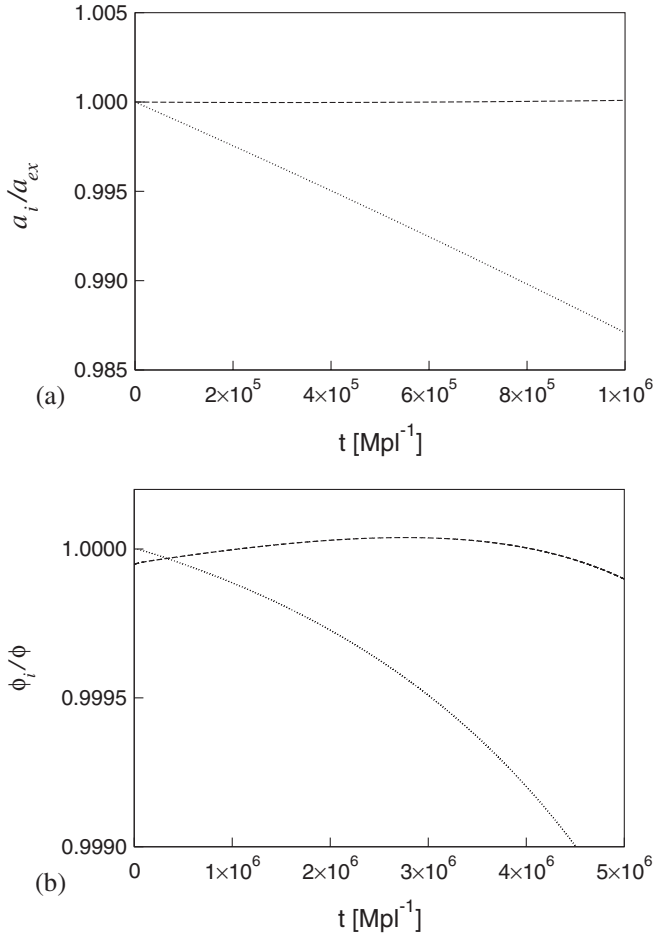

FIG. 3. (a) Ratio of the fit and slow roll to the exact solution for $a(t)$: a_i/a and (b) ratio of the fit and slow roll to the exact solution for $\phi(t)$: ϕ_i/ϕ, in the chaotic inflationary model $\frac{1}{2}m^2\phi^2$. Dashed lines: fitting; dotted lines: slow-roll approximation.

$$U_k \to A_k\sqrt{a(t)}z_{\rm S}(t), \qquad kt \to \infty, \tag{20}$$

$$U_k \to \sqrt{\frac{a(t)}{2k}}\exp[-ik\eta(t)], \qquad kt \to 0. \tag{21}$$

The asymptotic conditions (20) and (21) also hold for V_k.

We now proceed to write the explicit equations for quadratic chaotic inflation. From Eqs. (18) and (19), with Eqs. (11) and (12) we obtain

$$R_{\rm S}(k,t) = \frac{k^2}{a_i^2}\exp[-2t(\alpha-\beta t)] - \frac{[32\beta^2+9(\alpha-2\beta t)^4]}{4(\alpha-2\beta t)^2} - 3\beta, \tag{22}$$

$$R_{\rm T}(k,t) = \frac{k^2}{a_i^2}\exp[-2t(\alpha-\beta t)] - \frac{9}{4}(\alpha-2\beta t)^2 + 3\beta. \tag{23}$$

In order to apply the asymptotic condition (21), we use the relation between η and t, which is given by

$$\eta = \frac{\sqrt{\pi}}{2a_i\sqrt{\beta}}\exp\left(\frac{-\alpha^2}{4\beta}\right)\left[\mathrm{Erfi}\left(\frac{-\alpha+2\beta t}{2\sqrt{\beta}}\right) + \mathrm{Erfi}\left(\frac{\alpha-2\beta t_0}{2\sqrt{\beta}}\right)\right], \tag{24}$$

where $\mathrm{Erfi}(z)$ is the imaginary error function [29]. Since the conformal time η is defined up to an integration constant, the lower limit t_i of the integral

$$d\eta = \int_{t_i}^{t}\frac{dt}{a(t)}, \tag{25}$$

is chosen in order to make $\eta = 0$ at the end of the inflationary epoch, i.e., $t_i = 10^7 M_{\rm Pl}^{-1}$. The dependence of η on t is shown in Fig. 4. We can observe that as

$$-k\eta \to 0 \Rightarrow kt \to \infty, \tag{26}$$

$$-k\eta \to \infty \Rightarrow kt \to 0. \tag{27}$$

Equations (16) and (17), where $R_{\rm S}(k,t)$ and $R_{\rm T}(k,t)$ are given by Eqs. (22) and (23), do not possess exact analytic solution. In order to solve the differential equations governing the scalar and tensor perturbations in the physical time t, we use the fifth-order phase-integral approximation and compare these results with the slow roll and uniform approximation.

D. Phase-integral approximation

In order to solve Eqs. (16) and (17) with the help of the phase-integral approximation, we choose the following base functions Q for the scalar and tensor perturbations:

$$Q_{\rm S}^2(k,t) = R_{\rm S}(k,t), \tag{28}$$

$$Q_{\rm T}^2(k,t) = R_{\rm T}(k,t), \tag{29}$$

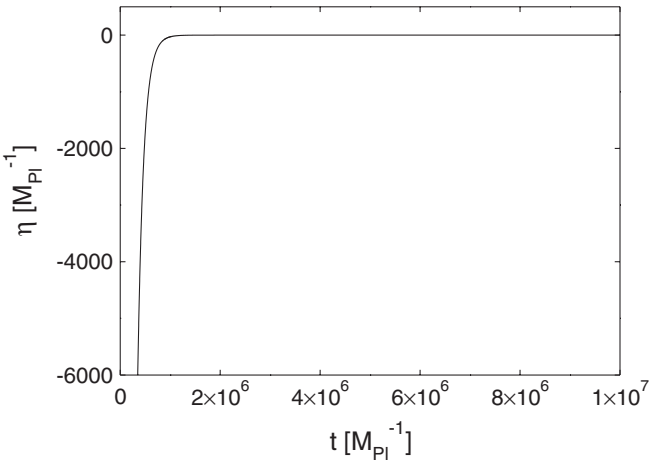

FIG. 4. Behavior of η as a function of the physical time t for the chaotic inflationary model $\frac{1}{2}m^2\phi^2$.

where $R_S(k,t)$ and $R_T(k,t)$ are given by Eqs. (22) and (23), respectively. Using this selection, the phase-integral approximation is valid as $kt \to \infty$, the limit where we should impose the condition (20), where the validity condition $\mu \ll 1$ holds. The selection, given in Eq. (28), makes the first-order phase-integral approximation coincide with the WKB solution. The base functions $Q_S(k,t)$ and $Q_T(k,t)$ possess turning points $t_{ret} = \tau_S = 1.380\,96 \times 10^6 M_{Pl}^{-1}$ and $t_{ret} = \tau_T = t = 1.381\,96 \times 10^6 M_{Pl}^{-1}$, respectively, for the mode $k = 1.369h$ Mpc^{-1}. The turning point represents the horizon. There are two ranges in which to define the solution. To the left of the turning point $0 < t < t_{ret}$ we have the classically permitted region $Q^2_{S,T}(k,t) > 0$ and to the right of the turning point $t > t_{ret}$ corresponding to the classically forbidden region $Q^2_{S,T}(k,t) < 0$, such as it is shown in Figs. 5(a) and 6(a).

The mode k equations for the scalar and tensor perturbations (16) and (17) in the phase-integral approximation have two solutions: For $0 < t < t_{ret}$

$$u_k^{pi}(t) = \frac{c_1}{\sqrt{a(t)}}|q_S^{-1/2}(k,t)|\cos\left[|\omega_S(k,t)| - \frac{\pi}{4}\right] + \frac{c_2}{\sqrt{a(t)}}|q_S^{-1/2}(k,t)|\cos\left[|\omega_S(k,t)| + \frac{\pi}{4}\right], \quad (30)$$

$$v_k^{pi}(t) = \frac{d_1}{\sqrt{a(t)}}|q_T^{-1/2}(k,t)|\cos\left[|\omega_T(k,t)| - \frac{\pi}{4}\right] + \frac{d_2}{\sqrt{a(t)}}|q_T^{-1/2}(k,t)|\cos\left[|\omega_T(zk,t| + \frac{\pi}{4}\right], \quad (31)$$

and for $t > t_{ret}$

$$u_k^{pi}(t) = \frac{c_1}{2\sqrt{a(t)}}|q_S^{-1/2}(k,t)|\exp[-|\omega_S(k,t)|] + \frac{c_2}{\sqrt{a(t)}}|q_S^{-1/2}(k,t)|\exp[|\omega_S(k,t)|], \quad (32)$$

$$v_k^{pi}(z) = \frac{d_1}{2\sqrt{a(t)}}|q_T^{-1/2}(k,t)|\exp[-|\omega_T(k,t)|] + \frac{d_2}{\sqrt{a(t)}}|q_T^{-1/2}(k,t)|\exp[|\omega_T(k,t)|]. \quad (33)$$

Using the phase-integral approximation up to fifth order ($2N + 1 = 5 \to N = 2$), we have that $q_S(k,t)$ and $q_T(k,t)$ can be expanded in the form

$$q_S(k,t) = \sum_{n=0}^{2} Y_{2n_S}(k,t)Q_S(k,t) = [Y_{0_S}(k,t) + Y_{2_S}(k,t) + Y_{4_S}(k,t)]Q_S(k,t), \quad (34)$$

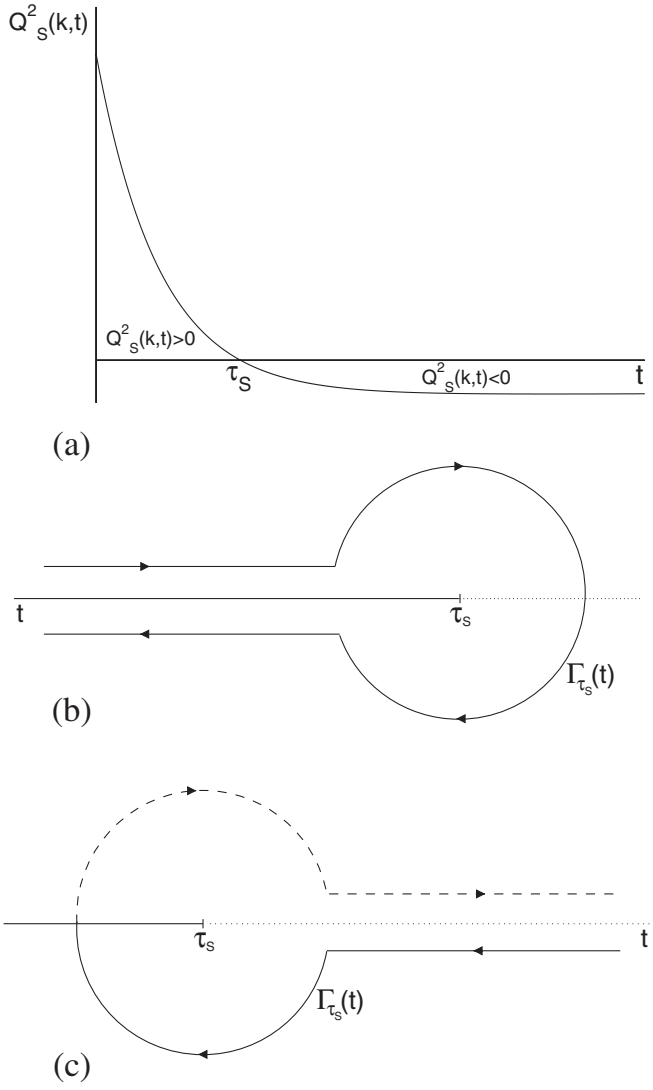

FIG. 5. (a) Behavior of the function $Q_S^2(k,t)$; (b) contour of integration $\Gamma_{\tau_S}(t)$ for $0 < t < \tau_S$; (c) contour of integration $\Gamma_{\tau_S}(t)$ for $t > \tau_S$. The dashed line indicates the part of the path on the second Riemann sheet.

$$q_T(k,t) = \sum_{n=0}^{2} Y_{2n_T}(k,t)Q_T(k,t) = [Y_{0_T}(k,t) + Y_{2_T}(k,t) + Y_{4_T}(k,t)]Q_T(k,t). \quad (35)$$

In order to compute $q_S(k,t)$ and $q_T(k,t)$, we compute $Y_{2_S}(k,t)$, $Y_{4_S}(k,t)$, $Y_{2_T}(k,t)$, $Y_{4_T}(k,t)$ and the required functions $\varepsilon_{0_S}(k,t)$, $\varepsilon_{2_S}(k,t)$, $\varepsilon_{0_T}(k,t)$, and $\varepsilon_{2_T}(k,t)$. The expressions (34) and (35) give a fifth-order approximation for $q_S(k,t)$ and $q_T(k,t)$. In order to compute $\omega_S(k,t)$ and $\omega_T(k,t)$ we make a contour integration following the path indicated in Figs. 5(b), 5(c), 6(b), and 6(c)

$$\omega_S(k,t) = \omega_{0_S}(k,t) + \sum_{n=1}^{2} \omega_{2n_S}(k,t), \quad (36)$$

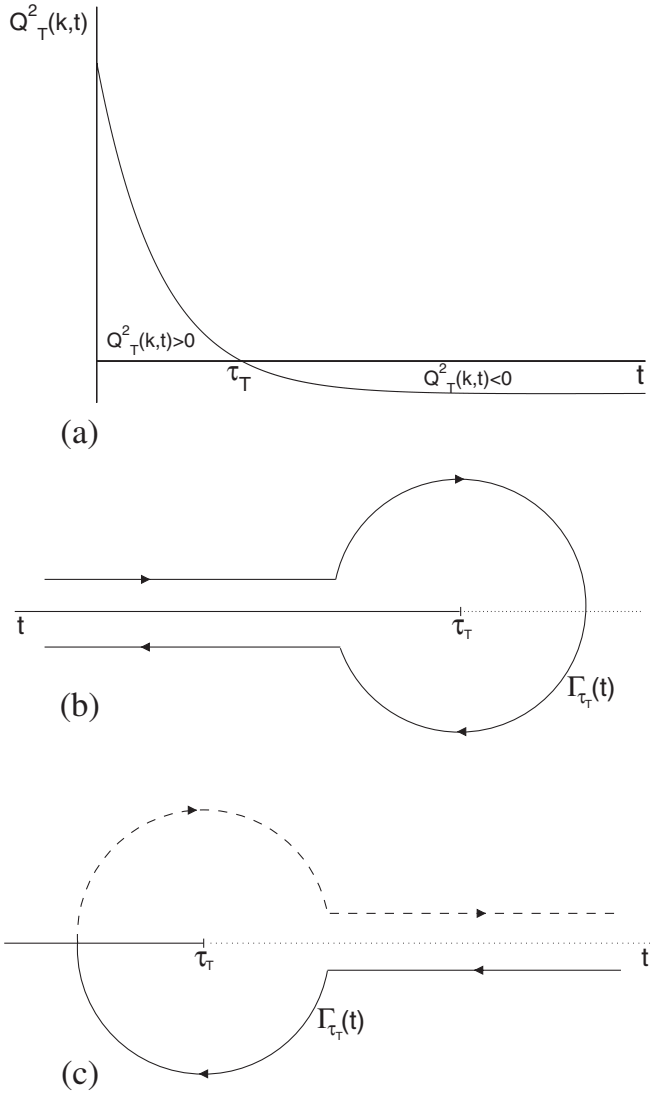

FIG. 6. (a) Behavior of $Q_{\mathrm{T}}^2(k,t)$; (b) contour of integration $\Gamma_{\tau_{\mathrm{T}}}(t)$ for $0 < t < \tau_{\mathrm{T}}$; (c) contour of integration $\Gamma_{\tau_{\mathrm{T}}}(t)$ for $t > \tau_{\mathrm{T}}$. The dashed line indicates the part of the path on the second Riemann sheet.

$$= \int_{\tau_{\mathrm{S}}}^{t} Q_{\mathrm{S}}(k,t)dt + \frac{1}{2}\sum_{n=1}^{2}\int_{\Gamma_{\tau_{\mathrm{S}}}} Y_{2n_{\mathrm{S}}}(k,t)Q_{\mathrm{S}}(k,t)dt, \quad (37)$$

$$= \int_{\tau_{\mathrm{S}}}^{t} Q_{\mathrm{S}}(k,t)dt + \frac{1}{2}\sum_{n=1}^{2}\int_{\Gamma_{\tau_{\mathrm{S}}}} f_{2n_{\mathrm{S}}}(k,t)dt, \quad (38)$$

$$\omega_{\mathrm{T}}(k,t) = \omega_{0_{\mathrm{T}}}(k,t) + \sum_{n=1}^{2}\omega_{2n_{\mathrm{T}}}(k,t), \quad (39)$$

$$= \int_{\tau_{\mathrm{T}}}^{t} Q_{\mathrm{T}}(k,t)dt + \frac{1}{2}\sum_{n=1}^{2}\int_{\Gamma_{\tau_{\mathrm{T}}}} Y_{2n_{\mathrm{T}}}(k,t)Q_{\mathrm{T}}(k,t)dt, \quad (40)$$

$$= \int_{\tau_{\mathrm{S}}}^{t} Q_{\mathrm{T}}(k,t)dz + \frac{1}{2}\sum_{n=1}^{2}\int_{\Gamma_{\tau_{\mathrm{T}}}} f_{2n_{\mathrm{T}}}(k,t)dt, \quad (41)$$

where

$$f_{2n_{\mathrm{S}}}(k,t) = Y_{2n_{\mathrm{S}}}(k,t)Q_{\mathrm{S}}(k,t), \quad (42)$$

$$f_{2n_{\mathrm{T}}}(k,t) = Y_{2n_{\mathrm{T}}}(k,t)Q_{\mathrm{T}}(k,t). \quad (43)$$

The functions $f_{2n_{\mathrm{S}}}(k,t)$ and $f_{2n_{\mathrm{T}}}(k,t)$ have the following functional dependence:

$$f_{2_{\mathrm{S}}}(k,t) = A(k,t)(t-\tau_{\mathrm{S}})^{-5/2}, \quad (44)$$

$$f_{4_{\mathrm{S}}}(k,t) = B(k,t)(t-\tau_{\mathrm{S}})^{-11/2}, \quad (45)$$

$$f_{2_{\mathrm{T}}}(k,t) = C(k,t)(t-\tau_{\mathrm{T}})^{-5/2}, \quad (46)$$

$$f_{4_{\mathrm{T}}}(k,t) = D(k,t)(t-\tau_{\mathrm{T}})^{-11/2}, \quad (47)$$

where the functions $A(k,t)$ and $B(k,t)$ are regular at τ_{S} and the functions $C(k,t)$, $D(k,t)$ are regular at τ_{T}. With the help of the functions (44)–(47) we compute the integrals for ω_{2n} up to $N = 4$ using the contour indicated in Figs. 5(b), 5(c), 6(b), and 6(c). The expressions for ω_{2n} permit one to obtain the fifth-order phase-integral approximation of the solution to the equations for scalar (16) and tensor (17) perturbations. The constants c_1, c_2, d_1, and d_2 are obtained using the limit $kt \to 0$ of the solutions on the left side of the turning point (30) and (31), and are given by the expressions

$$c_1 = -ic_2, \quad (48)$$

$$c_2 = \frac{e^{-i(\pi/4)}}{\sqrt{2}}e^{-i[k\eta(0)+|\omega_{0_{\mathrm{S}}}(k,0)|]}, \quad (49)$$

$$d_1 = -id_2, \quad (50)$$

$$d_2 = \frac{e^{-i(\pi/4)}}{\sqrt{2}}e^{-i[k\eta(0)+|\omega_{0_{\mathrm{T}}}(k,0)|]}. \quad (51)$$

In order to compute the scalar and tensor power spectra, we need to calculate the limit as $kt \to \infty$ of the growing part of the solutions on the right side of the turning point given by Eqs. (32) and (33) for scalar and tensor perturbations, respectively,

$$P_{\mathrm{S}}(k) = \lim_{-kt\to\infty}\frac{k^3}{2\pi^2}\left|\frac{u_k^{\mathrm{pi}}(t)}{z_{\mathrm{S}}(t)}\right|^2, \quad (52)$$

$$P_{\mathrm{T}}(k) = \lim_{-kt\to\infty}\frac{k^3}{2\pi^2}\left|\frac{v_k^{\mathrm{pi}}(t)}{a(t)}\right|^2. \quad (53)$$

E. Uniform approximation

We want to obtain an approximate solution to the differential equations (16) and (17) in the range where $Q_{\rm S}^2(k,t)$ and $Q_{\rm T}^2(k,t)$ have a simple root at $t_{\rm ret}=\tau_{\rm S}$ and $t_{\rm ret}=\tau_{\rm T}$, respectively, so that $Q_{\rm S,T}^2(k,t)>0$ for $0<t<t_{\rm ret}$ and $Q_{\rm S,T}^2(k,t)<0$ for $t>t_{\rm ret}$ as depicted in Figs. 5(a) and 6(a). Using the uniform-approximation method [13,18–20], we obtain that for $0<t<t_{\rm ret}$ we have

$$U_k(k,t)=\left[\frac{\rho_1(k,t)}{Q_{\rm S}^2(k,t)}\right]^{1/4}\{C_1A_i[-\rho_1(k,t)]+C_2B_i[-\rho_1(k,t)]\},\tag{54}$$

$$V_k(k,t)=\left[\frac{\rho_1(k,t)}{Q_{\rm T}^2(k,t)}\right]^{1/4}\{C_1A_i[-\rho_1(k,t)]+C_2B_i[-\rho_1(k,t)]\},\tag{55}$$

$$\frac{2}{3}[\rho_1(k,t)]^{3/2}=\int_t^{t_{\rm ret}}[Q_{\rm S,T}^2(k,t)]^{1/2}dt,\tag{56}$$

where C_1 and C_2 are two constants to be determined with the help of the boundary conditions (21). For $t>t_{\rm ret}$

$$U_k(k,t)=\left[\frac{-\rho_{\rm r}(k,t)}{Q_{\rm S}^2(k,t)}\right]^{1/4}\{C_1A_i[\rho_{\rm r}(k,t)]+C_2B_i[\rho_{\rm r}(k,t)]\},\tag{57}$$

$$V_k(k,t)=\left[\frac{-\rho_{\rm r}(k,t)}{Q_{\rm T}^2(k,t)}\right]^{1/4}\{C_1A_i[\rho_{\rm r}(k,t)]+C_2B_i[\rho_{\rm r}(k,t)]\},\tag{58}$$

$$\frac{2}{3}[\rho_{\rm r}(k,t)]^{3/2}=\int_{t_{\rm ret}}^t[-Q_{\rm S,T}^2(k,t)]^{1/2}dt.\tag{59}$$

For the computation of the power spectrum we need to take the limit $kt\to\infty$ of the solutions (57) and (58). In this limit we have

$$u_k^{\rm ua}(t)\to\frac{C}{\sqrt{2a(t)}}[-Q_{\rm S}^2(k,t)]^{-1/2}\times\left\{\frac{1}{2}\exp\left(-\int_{\tau_{\rm S}}^t[-Q_{\rm S}^2(k,t)]^{1/2}dt\right)+i\exp\left(\int_{\tau_{\rm S}}^t[-Q_{\rm S}^2(k,t)]^{1/2}dt\right)\right\},\tag{60}$$

$$v_k^{\rm ua}(t)\to\frac{C}{\sqrt{2a(t)}}[-Q_{\rm T}^2(k,t)]^{-1/2}\times\left\{\frac{1}{2}\exp\left(-\int_{\tau_{\rm T}}^t[-Q_{\rm T}^2(k,t)]^{1/2}dt\right)+i\exp\left(\int_{\tau_{\rm T}}^t[-Q_{\rm T}^2(k,t)]^{1/2}dt\right)\right\},\tag{61}$$

where C is a phase factor. Notice that Eqs. (60) and (61) are identical to Eqs. (32) and (33) obtained in the first-order phase-integral approximation. Using Eqs. (11) and (13) and the growing part of the solutions (60) and (61) one can compute the scalar and tensor power spectrum using the uniform-approximation method,

$$P_{\rm S}(k)=\lim_{-kt\to\infty}\frac{k^3}{2\pi^2}\left|\frac{u_k^{\rm ua}(t)}{z_{\rm S}(t)}\right|^2,\tag{62}$$

$$P_{\rm T}(k)=\lim_{-kt\to\infty}\frac{k^3}{2\pi^2}\left|\frac{v_k^{\rm ua}(t)}{a(t)}\right|^2.\tag{63}$$

We also use the second-order improved uniform approximation for the power spectrum [14],

$$\tilde{P}_{\rm S,T}(k)=P_{\rm S,T}(k)[\Gamma^*(\bar{\nu}_{\rm S,T})],\tag{64}$$

where $\bar{\nu}_{\rm S,T}$ is the turning point for the scalar or tensor power spectrum and

$$\Gamma^*(\nu)\equiv 1+\frac{1}{12\nu}+\frac{1}{288\nu}-\frac{139}{51840\nu}+\cdots.\tag{65}$$

F. Slow-roll approximation

The scalar and tensor power spectra in the slow-roll approximation to second order are given by the expressions [9,30]

$$P_{\rm S}^{\rm sr}(k)\simeq\left[1+(4c-2)\epsilon_1+2c\delta_1+\left(3c^2+2c-22+\frac{29\pi^2}{12}\right)\epsilon_1\delta_1+\left(3c^2-4+\frac{5\pi^2}{12}\right)\delta_1^2+\left(-c^2+\frac{\pi^2}{12}\right)\delta_2\right]\left(\frac{H}{2\pi}\right)^2\left(\frac{H}{\dot{\phi}}\right)^2\Bigg|_{k=aH},\tag{66}$$

$$P_{\rm T}^{\rm sr}(k)\simeq\left[1+(2c-2)\epsilon_1+\left(2c^2-2c-3+\frac{\pi^2}{2}\right)\epsilon_1^2+\left(-c^2+2c-2+\frac{\pi^2}{12}\right)\epsilon_2\right]\left(\frac{H}{2\pi}\right)^2\Bigg|_{k=aH},\tag{67}$$

where b is the Euler constant, $2-\ln 2-b\simeq 0.7296$ and $\ln 2+b-1\simeq 0.2704$, and

$$\epsilon_1=\frac{\dot{H}}{H^2}=\frac{1}{1+2N_*},\tag{68}$$

$$\epsilon_2=\frac{1}{H}\frac{d\epsilon_1}{dt}=\frac{2}{(1+2N_*)^2},\tag{69}$$

$$\delta_n\equiv\frac{1}{H^n\dot{\phi}}\frac{d^{n+1}\phi}{dt^{n+1}}\to\delta_1=\delta_2=0.\tag{70}$$

The spectral indices in the slow-roll approximation are

$$n_{\rm S}^{\rm sr}(k) \simeq 1 - 4\epsilon_1 - 2\delta_1 + (8c - 8)\epsilon_1^2 + (10c - 6)\epsilon_1\delta_1, \tag{71}$$

$$n_{\rm T}^{\rm sr}(k) \simeq -2\epsilon_1 - 2\epsilon_1^2 + (2\alpha - 2)\epsilon_2. \tag{72}$$

The expressions (66), (67), (71), and (72) depend explicitly on time. In order to compute the scalar and tensor power spectra we need to obtain the dependence on the variable k. For a given value of k ($0.0001\ \mathrm{Mpc}^{-1} \leq k \leq 15\ \mathrm{Mpc}^{-1}$) we obtain t_* from the relation $k = aH$. Thus, for each k one obtains a value of t that we substitute into N_* and Eqs. (66), (67), (71), and (72).

G. Numerical solution

We integrate on the physical time t the Eqs. (16) and (17) governing the scalar and tensor perturbations using the predictor-corrector Adams method of order 12 [28], and solve two differential equations, one for the real part and another for the imaginary parts U_k and V_k. Two initial conditions are needed in each case $U_k(t_i)$, $U_k'(t_i)$, $V_k(t_i)$, and $V_k'(t_i)$, which can be obtained from the third-order phase-integral approximation. We start the numerical integration at t_i calculated at 25 oscillations before reaching the turning point $t_{\rm ret}$ [31]. We call this procedure ICs phi3. Figures 7–9 compare the numerical solution with the fifth-

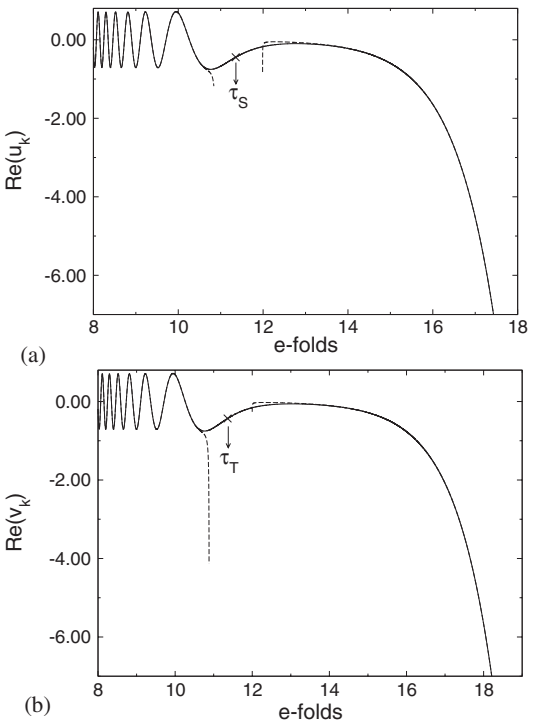

FIG. 7. (a) $\mathrm{Re}(u_k)$ and (b) $\mathrm{Re}(v_k)$ versus the number of e-folds for the chaotic inflationary model $\frac{1}{2}m^2\phi^2$. Solid lines: numerical solution (ICs phi3); dashed lines: fifth-order phase-integral approximation.

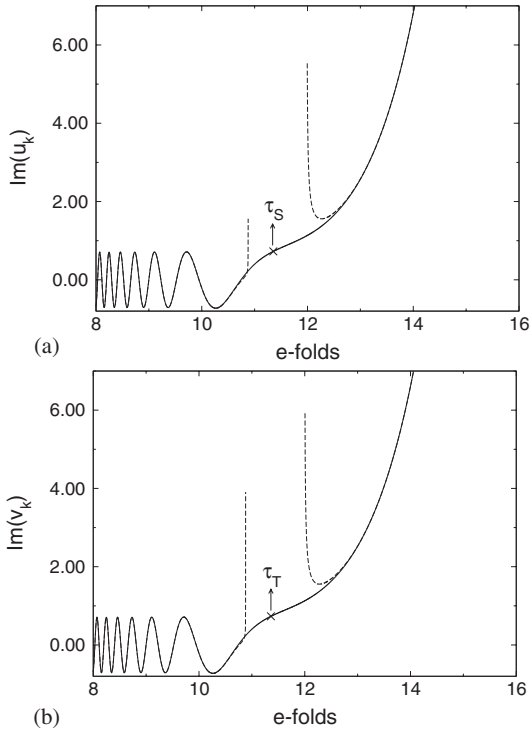

FIG. 8. (a) $\mathrm{Im}(u_k)$ and (b) $\mathrm{Im}(v_k)$ versus the number of e-folds for the chaotic inflationary model $\frac{1}{2}m^2\phi^2$. Solid lines: numerical result (ICs phi3); dashed lines: fifth-order phase-integral approximation.

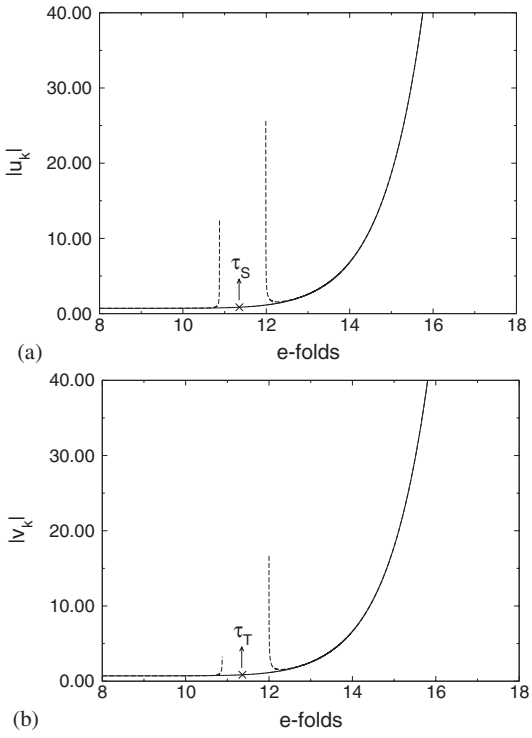

FIG. 9. (a) $|u_k|$ and (b) $|v_k|$ versus the number of e-folds for the chaotic inflationary model $\frac{1}{2}m^2\phi^2$. Solid lines: Numerical result (ICs phi3); dashed lines: fifth-order phase-integral approximation.

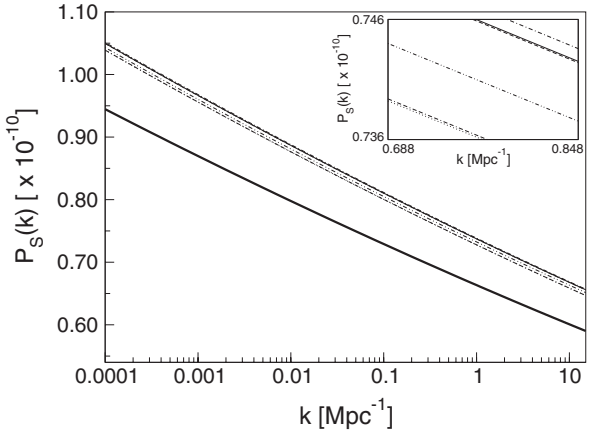

FIG. 10. $P_S(k)$ for the chaotic inflationary $\frac{1}{2}m^2\phi^2$ model. Thin solid line: numerical result (ICs phi3); dot-dashed line: third-order phase-integral approximation; dashed line: fifth-order phase-integral approximation; thick solid line: first-order phase-integral approximation, WKB, and first-order uniform approximation; dashed double-dots line: second-order improved uniform approximation; double-dashed dot line: second-order slow-roll approximation; dotted line: first-order slow-roll approximation. The inset is an enlargement of the figure.

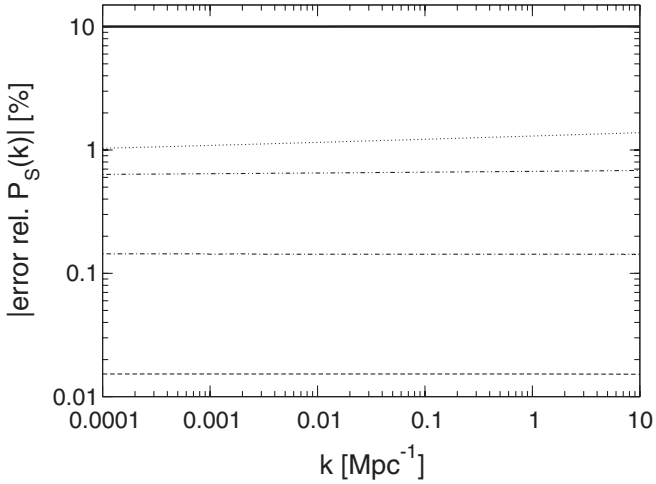

FIG. 11. Relative error for $P_S(k)$ for the chaotic inflationary $\frac{1}{2}m^2\phi^2$ model. Dot-dashed line: third-order phase-integral approximation; dashed line: fifth-order phase-integral approximation; thick solid line: first-order phase-integral approximation, WKB, and first-order uniform approximation; dashed double-dots line: second-order improved uniform approximation; dotted line: first- and second-order slow-roll approximation. The inset is an enlargement of the figure.

order phase-integral approximation for $\mathrm{Re}(u_k)$, $\mathrm{Im}(u_k)$, $|u_k|$, $\mathrm{Re}(v_k)$, $\mathrm{Im}(v_k)$, and $|v_k|$. The figures are plotted against the number of e-folds N. The solid lines correspond to the numerical solutions (ICs phi3), and the dashed lines correspond to the fifth-order phase-integral approximations. In each case the turning points τ_S and τ_T are indicated with an arrow. We stop the numerical computation of $P_S(k)$ and $P_T(k)$ at $t = 5.00 \times 10^6 M_{\mathrm{Pl}}^{-1}$, after the mode leaves the horizon, where u_k/z_S and v_k/a are approximately constant. Notice that the expressions for fitting (11) and (12) are valid in the aforementioned time scales; therefore we can use them for computing the scalar $P_S(k)$ and tensor $P_T(k)$ power spectra.

H. Results

For the chaotic $\frac{1}{2}m^2\phi^2$ inflationary model, we want to compare the scalar and tensor power spectra and the spectral indices for different values of k calculated using the third- and fifth-order phase-integral approximation with the numerical result (ICs phi3), the first- and second-order slow-roll approximation and the first- and second-order uniform-approximation method. First we analyze the results for the scalar $P_S(k)$ and tensor $P_T(k)$ power spectra shown in Figs. 10 and 12.

Table I shows the value of $P_S(k)$, $P_T(k)$, $n_S(k)$, and $n_T(k)$ using each method of approximation at the WMAP pivot scale. It can be observed that the best value is obtained with

TABLE I. Value of $P_S(k)$, $P_T(k)$, $n_S(k)$, and $n_T(k)$ obtained with different approximation methods for the chaotic inflationary model $\frac{1}{2}m^2\phi^2$ for the mode $k = 0.05$ Mpc^{-1}.

	num[a]	phi3[b]	phi5[c]	sr1[d]	sr2[e]	phi1,[f] WKB,[g] ua1[h]	ua2[i]
$P_S(k) \times 10^{-11}$	8.330 0	8.341 9	8.328 7	8.228 2	8.229 9	7.494 6	8.275 2
$P_T(k) \times 10^{-12}$	1.610 9	1.613 2	1.610 6	1.604 7	1.604 9	1.448 6	1.600 4
$n_S(k)$	0.960 473	0.960 472	0.964 73	0.960 700	0.960 491	0.960 453	0.960 486
$n_T(k)$	−0.019 965	−0.019 982	−0.019 965	−0.019 650	−0.019 948	−0.020 000	−0.019 984

[a]Numerical.
[b]Third-order phase-integral approximation.
[c]Fifth-order phase-integral approximation.
[d]First-order slow-roll approximation.
[e]Second-order slow-roll approximation.
[f]First-order phase-integral approximation.
[g]WKB approximation.
[h]First-order uniform approximation.
[i]Second-order improved uniform approximation.

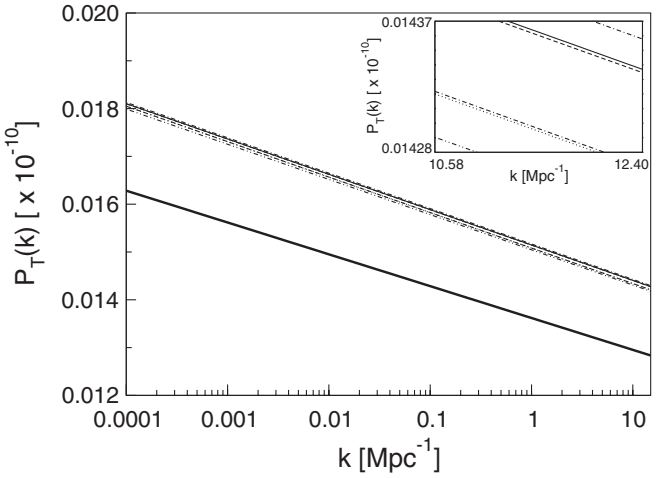

FIG. 12. $P_T(k)$ for the chaotic inflationary $\frac{1}{2}m^2\phi^2$ model. Thin solid line: numerical result (ICs phi3); dot-dashed line: third-order phase-integral approximation; dashed line: fifth-order phase-integral approximation; thick solid line: first-order phase-integral approximation, WKB, and first-order uniform approximation; dashed double-dots line: second-order improved uniform approximation; double-dashed dot line: second-order slow-roll approximation; dotted line: first-order slow-roll approximation. The inset is an enlargement of the figure.

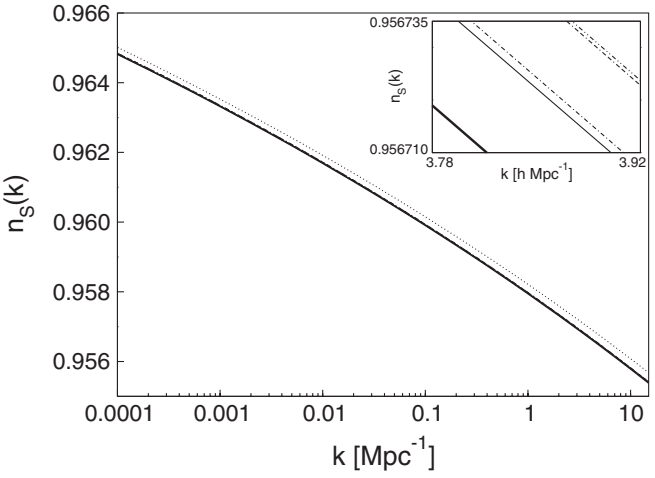

FIG. 14. $n_S(k)$ for the chaotic inflationary $\frac{1}{2}m^2\phi^2$ model. Thin solid line: numerical result (ICs phi3) and fifth-order phase-integral approximation; dot-dashed line: third-order phase-integral approximation; thick solid line: first-order phase-integral approximation, WKB, and first-order uniform approximation; dashed double-dots line: second-order improved uniform approximation; double-dashed dot line: second-order slow-roll approximation; dotted line: first-order slow-roll approximation. The inset is an enlargement of the figure.

the fifth-order phase-integral approximation. It should be noticed that the slow-roll approximation works well since the parameters ϵ_1, ϵ_2, and δ_n are small.

Figures 11 and 13 show the relative error with respect to the numerical result that is obtained using the expression

$$\text{error rel. } P_{S,T}(k) = \frac{[P_{S,T}^{\text{approx}}(k) - P_{S,T}^{\text{num}}(k)]}{P_{S,T}^{\text{num}}(k)} \times 100. \quad (73)$$

The first-order phase-integral approximation, the WKB, and the first-order uniform approximation give the same

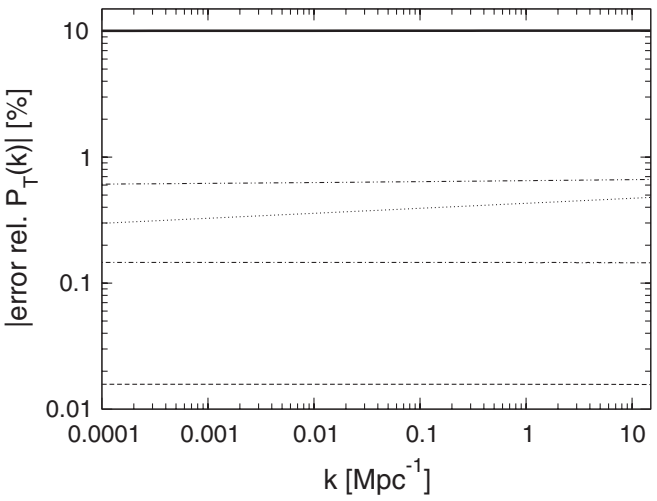

FIG. 13. Relative error for $P_T(k)$ for the chaotic inflationary $\frac{1}{2}m^2\phi^2$ model. Dot-dashed line: third-order phase-integral approximation; dashed line: fifth-order phase-integral approximation; thick solid line: first-order phase-integral approximation, WKB, and first-order uniform approximation; dashed double-dots line: second-order improved uniform approximation; dotted line: first- and second-order slow-roll approximation. The inset is an enlargement of the figure.

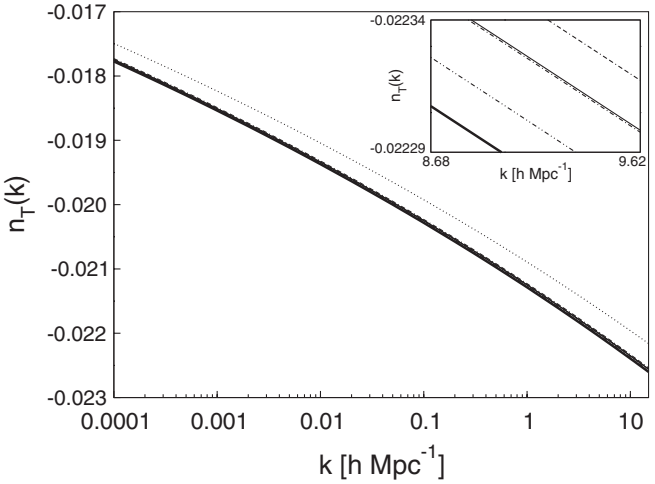

FIG. 15. $n_T(k)$ for the chaotic inflationary $\frac{1}{2}m^2\phi^2$ model. Thin solid line: numerical result (ICs phi3) and fifth-order phase-integral approximation; dot-dashed line: third-order phase-integral approximation; thick solid line: first-order phase-integral approximation, WKB, and first-order uniform approximation; dashed double-dots line: second-order improved uniform approximation; double-dashed dot line: second-order slow-roll approximation; dotted line: first-order slow-roll approximation. The inset is an enlargement of the figure.

result, and deviate from the numerical result in 10%. The second-order improved uniform approximation gives an error of 0.6%. With the first- and second-order slow-roll approximations we have an error of 1% for $P_S(k)$ and of 0.4% for $P_T(k)$. Using the third-order phase-integral approximation the error gives 0.15%, whereas the fifth-order phase integral reduces to 0.015% in both cases. Figures 14 and 15 show the results for the spectral indices $n_S(k)$ and $n_T(k)$, respectively.

III. CONCLUSION

The results reported in this article show that, in comparison with other approximation methods, the phase-integral approach gives very good results for the scalar and tensor spectra in the quadratic inflationary model. The phase-integral approximation gives very accurate results as soon as the integral $\mu(z, z_0)$ is small. Figures 7–9 show that the phase-integral approximation fails in the vicinity of the turning point $-\nu$ range where the μ integral diverges. The selection of the base function $Q(z)$ guarantees that $\mu \ll 1$ far from the turning point at any order of approximation. Since the scalar and tensor power spectra as well as the spectral indices are evaluated as $-k\eta \to 0$, the limit is taken far from the horizon (turning point); therefore their computation is not affected by the presence of the turning point.

Since the WKB method can be regarded as a first-order approximation of the phase-integral approximation with $Q^2(z) = R(z)$, it should be expected that the phase-integral method works in those cases where the WKB method gives good estimates and slow roll fails. That is the case where inflation is generated by a chaotic potential with a step [15,32]. The good agreement between the numerical results and those obtained with the phase-integral approximation shows that the phase-integral method is a very useful approximation tool for computing the scalar and tensor power spectra in a wide range of inflationary scenarios.

ACKNOWLEDGMENTS

C. R. wishes to express her gratitude to Carlos Cunha for enlightening discussions and for his help in the implementation of the numerical code for solving the perturbation equations. We thank Dr. Ernesto Medina for reading and improving the manuscript. This work was partially supported by FONACIT under Project No. G-2001000712.

[1] E. Komatsu, J. Dunkley, M. R. Nolta, C. L. Bennet, B. Gold, G. Hinshaw, N. Jarosik, D. Larson, M. Limon, L. Page, D. N. Spergel, M. Halpern, R. S. Hill, A. Kogut, S. S. Meyer, G. S. Tucker, J. L. Weiland, E. Wollack, and E. L. Wright, Astrophys. J. **180**, 330 (2009).
[2] D. N. Spergel, R. Bean, O. Doré, M. R. Nolta, V. L. Bennett, G. Hinshaw, N. Jarosik, E. Komatsu, L. Page, H. Peiris, L. Verde, V. Barnes, M. Halpern, R. S. Hill, A. Kogut, M. Limon, S. S. Meyer, N. Odegard, G. S. Tucker, J. L. Weiland, E. Wollack, and E. L. Wright, Astrophys. J. **170**, 377 (2007).
[3] D. N. Spergel, L. Verde, H. V. Peiris, E. Komatsu, M. R. Nolta, C. L. Bennett, M. Halpern, G. Hinshaw, N. Jarosik, A. Kogut, M. Limon, S. S. Meyer, L. Page, G. S. Tucker, J. L. Weiland, E. Wollack, and E. L. Wright, Astrophys. J. **148**, 175 (2003).
[4] W. H. Kinney, E. W. Kolb, A. Melchiorri, and A. Riotto, Phys. Rev. D **78**, 087302 (2008).
[5] E. D. Stewart and D. H. Lyth, Phys. Lett. B **302**, 171 (1993).
[6] R. Langer, Phys. Rev. **51**, 669 (1937).
[7] J. Martin and D. J. Schwarz, Phys. Rev. D **67**, 083512 (2003).
[8] R. Casadio, F. Finelli, M. Luzzi, and G. Venturi, Phys. Rev. D **71**, 043517 (2005).
[9] E. D. Stewart and J. Gong, Phys. Lett. B **510**, 1 (2001).
[10] R. Casadio, F. Finelli, M. Luzzi, and G. Venturi, Phys. Rev. D **72**, 103516 (2005).
[11] R. Casadio, F. Finelli, M. Luzzi, and G. Venturi, Phys. Lett. B **625**, 1 (2005).
[12] S. Habib, A. Heinen, K. Heitmann, G. Jungman, and C. Molina-París, Phys. Rev. D **70**, 083507 (2004).
[13] S. Habib, K. Heitmann, G. Jungman, and C. Molina-París, Phys. Rev. Lett. **89**, 281301 (2002).
[14] S. Habib, A. Heinen, K. Heitmann, and G. Jungman, Phys. Rev. D **71**, 043518 (2005).
[15] R. Casadio, F. Finelli, A Kamenshchik, M Luzzi, and G Venturi, J. Cosmol. Astropart. Phys. 04 (2006) 011.
[16] R. B. Dingle, Appl. Sci. Res. **5**, 345 (1956).
[17] S. C. Miller and R. H. Good, Phys. Rev. **91**, 174 (1953).
[18] M. V. Berry and K. E. Mount, Rep. Prog. Phys. **35**, 315 (1972).
[19] C. Rojas and V. M. Villalba, Phys. Rev. D **75**, 063518 (2007).
[20] V. M. Villalba and C. Rojas, J. Phys. Conf. Ser. **66**, 012034 (2007).
[21] N. Fröman and P. O. Fröman, *JWKB Approximation. Contribution to the Theory* (North-Holland, Amsterdam, 1965).
[22] N. Fröman and P. O. Fröman, *Phase-Integral Method. Allowing Nearlying Transition Points*, Springer Tracts in Natural Philosophy Vol. 40 (Springer, New York, 1996).
[23] N. Fröman and P. O. Fröman, *Physical Problems Solved by the Phase-Integral Method* (Cambridge University Press, Cambridge, England, 2002).
[24] A. D. Linde, JETP Lett. **38**, 176 (1983).
[25] A. D. Linde, Phys. Lett. **129B**, 177 (1983).
[26] A. R. Liddle and D. H. Lyth, *Cosmological Inflation and Large-Scale Structure* (Cambridge University Press, Cambridge, England, 2000).

[27] E. J. Copeland, *Inflation in the Early Universe and Today. The Early Universe and Observational Cosmology*, Lecture Notes in Physics Vol. 646 (Springer-Verlag, Berlin, 2004), p. 53.
[28] C. F. Gerald and P. O. Wheatley, *Applied Numerical Analysis* (Addison-Wesley, Reading, MA, 1984).
[29] M. Abramowitz and I. Stegun, *Handbook of Mathematical Functions* (Dover, New York, 1964).
[30] J. Gong, Classical Quantum Gravity **21** 5555 (2004).
[31] C. E. Cunha, Evolution of background and perturbation equations in single field inflation models, http://astro.uchicago.edu/~cunha/inflation/node7.htm, 2005.
[32] P. Hunt and S. Sarkar, Phys. Rev. D **70**, 103518 (2004).